Lévy flights and Lévy walks under stochastic resetting

Bartosz Żbik[*]
Faculty of Physics, Astronomy and Applied Computer Science, Jagiellonian University, Łojasiewicza 11, 30-348 Kraków, Poland

Bartłomiej Dybiec[†]
Institute of Theoretical Physics and Mark Kac Center for Complex Systems Research, Faculty of Physics, Astronomy and Applied Computer Science, Jagiellonian University, Łojasiewicza 11, 30-348 Kraków, Poland

(Received 27 November 2023; accepted 27 March 2024; published 22 April 2024)

Stochastic resetting is a protocol of starting anew, which can be used to facilitate the escape kinetics. We demonstrate that restarting can accelerate the escape kinetics from a finite interval restricted by two absorbing boundaries also in the presence of heavy-tailed, Lévy-type, α-stable noise. However, the width of the domain where resetting is beneficial depends on the value of the stability index α determining the power-law decay of the jump length distribution. For heavier (smaller α) distributions, the domain becomes narrower in comparison to lighter tails. Additionally, we explore connections between Lévy flights (LFs) and Lévy walks (LWs) in the presence of stochastic resetting. First of all, we show that for Lévy walks, the stochastic resetting can also be beneficial in the domain where the coefficient of variation is smaller than 1. Moreover, we demonstrate that in the domain where LWs are characterized by a finite mean jump duration (length), with the increasing width of the interval, the LWs start to share similarities with LFs under stochastic resetting.

DOI: 10.1103/PhysRevE.109.044147

I. INTRODUCTION

Since the pioneering works of Smoluchowski [1], Einstein [2], Langevin [3], Perrin [4], and Kramers [5], the study of Brownian motion and random phenomena has attracted steadily growing interest. The probabilistic explanation of the properties of Brownian motion boosted development of the theory of stochastic processes [6,7], increased our understanding of random phenomena [8], and opened studies of noise driven systems [9] and random walks [10–12].

The Wiener process [Brownian motion (BM)] is one of the simplest examples of continuous (time and space) random processes. Its mathematical properties nicely explain the observed properties of Brownian motion [13], e.g., the linear scaling of the mean-square displacement [4,14]. It can be extended in multiple ways, e.g., by assuming more general jump length distribution, introducing memory, or assuming finite propagation velocity. In that context, Lévy flights (LFs) [15,16] and Lévy walks (LWs) [17–19] are two archetypal types of random walks [10]. In the LFs, it is assumed that displacements are immediate and generated from a heavy-tailed, power-law distribution. At the same time, in the LWs, a random walker travels with a finite velocity v for random times distributed according to a power-law density.

The assumption that individual jump lengths follow a general α-stable density is supported by multiple experimental observations demonstrating the existence of more general than Gaussian fluctuations. Heavy-tailed, power-law fluctuations have been observed in a plenitude of experimental setups including, but not limited to, biological systems [20], dispersal patterns of humans and animals [21,22], search strategies [17,23], gaze dynamics [24], balance control [25,26], rotating flows [27], optical systems and materials [28,29], laser cooling [30], disordered media [31], and financial time series [32–34]. The properties of systems displaying heavy-tailed, non-Gaussian fluctuations are studied both experimentally [24,27,35] and theoretically [11,15,36–44]. Lévy flights have attracted considerable attention due to their well-known mathematical properties, e.g., self-similarity, infinite divisibility, and generalized central limit theorem. Therefore, the α-stable noises are broadly applied in diverse models displaying anomalous fluctuations or describing anomalous diffusion.

Stochastic resetting [45–47] is a protocol of starting anew, which can be applied (among others) to increase the efficiency of search strategies. In the simplest version, it assumes that the motion is started anew at random times, i.e., restarts are triggered temporally, making the times of starting over independent of the state of the system, e.g., position. Among multiple options, resets can be performed periodically (sharp resetting) [48] or at random time intervals following exponential (Poissonian resetting) [45] or a power-law [49] density. Starting anew can be also spatially induced [50]. Escape kinetics under stochastic resetting display universal properties [48,51] regarding relative fluctuations of first passage times as measured by the coefficient of variation (CV) and as such can also be treated in the unified approach [52]. Typically, it is assumed that the restarting is immediate and does not generate additional costs; however, options with finite return velocity [53,54], overheads [55–57], or soft (due to attracting force) resetting [58] are also explored.

[*]bartosz.zbik@student.uj.edu.pl
[†]bartlomiej.dybiec@uj.edu.pl

 ©2024 American Physical Society

Stochastic resetting has attracted considerable attention due to its strong connection with search strategies [23,59,60] and its ability to reduce the spread of particles [61–63], even in the case of partial resetting [64]. During the search, an individual or animal is interested in the minimization of the time needed to find a target, which in turn is related to the first passage problem [65]. In certain setups, due to long excursions in the wrong direction, i.e., to points distant from the target [66–69], the mean first passage time (MFPT) can diverge. In such cases, stochastic resetting is capable of turning the MFPT finite. Furthermore, it can optimize already finite MFPT [48,51]. Stochastic resetting is capable of minimization of the time to find a target when the coefficient of variation (the ratio between the standard deviation of the first passage times and the MFPT in the absence of stochastic resetting) is greater than unity [48,51].

Not surprisingly, the stochastic resetting is capable of minimizing the MFPT from a finite interval restricted by two absorbing boundaries [70]. As demonstrated in [71], in the case of escape from finite intervals restricted by two absorbing boundaries, the mean first passage times for Lévy flights and Lévy walks display similar scaling [71] as a function of the interval width. Therefore, one can study the properties of escape from finite intervals under the combined action of Lévy noise and stochastic resetting with special attention to verification if the properties of escape kinetics still bear some similarities with LWs under restarts.

The model under study is described in the next section (Sec. II). Section III analyzes properties of LWs on finite intervals under stochastic resetting and compares them with the properties of corresponding LFs. The manuscript closes with a summary and conclusions in Sec. IV.

II. MODEL AND RESULTS

The noise driven escape (from any domain of motion Ω) is a stochastic process; therefore, individual first passage times are not fixed but random. For first passage times, it is possible to calculate—the relative standard deviation—the coefficient of variation (CV) [48],

$$\mathrm{CV} = \frac{\sigma(t_{\mathrm{fp}})}{\langle t_{\mathrm{fp}}\rangle} = \frac{\sigma(t_{\mathrm{fp}})}{\mathcal{T}} = \frac{\sqrt{\mathcal{T}_2 - \mathcal{T}^2}}{\mathcal{T}} = \sqrt{\frac{\mathcal{T}_2}{\mathcal{T}^2} - 1}, \tag{1}$$

which is the ratio between the standard deviation $\sigma(t_{\mathrm{fp}})$ of the first passage times (FPT) t_{fp} and the mean first passage time $\mathcal{T} = \langle t_{\mathrm{fp}}\rangle$. In addition to statistical applications, the coefficient of variation plays a special role in the theory of stochastic resetting [48,51,70]. It provides a useful universal tool for assessing the potential effectiveness of stochastic restarting, which can be used to explore various types of setups under very general conditions. Typically, stochastic resetting can facilitate the escape kinetics in the domain where $\mathrm{CV} > 1$. Therefore, examination of the CV given by Eq. (1) (constrained by the fact that resets are performed to the same point from which the motion was started) can be a starting point for the exploration of the effectiveness of stochastic resetting.

The escape of a free particle from a finite interval $(-L, L)$ under the action of Lévy noise, i.e., escape of α-stable, Lévy-type process, can be characterized by the mean first passage time (MFPT) $\mathcal{T}$, which reads [72]

$$\mathcal{T}(x_0) = \frac{(L^2 - |x_0|^2)^{\alpha/2}}{\Gamma(1+\alpha)\sigma^\alpha} = \frac{(1 - |x_0/L|^2)^{\alpha/2}}{\Gamma(1+\alpha)} \times \frac{L^\alpha}{\sigma^\alpha}, \tag{2}$$

and the second moment $\mathcal{T}_2 = \langle t_{\mathrm{fp}}^2\rangle$ given by [72]

$$\mathcal{T}_2(x_0) = \frac{\alpha L^\alpha}{[\Gamma(1+\alpha)\sigma^\alpha]^2} \times \int_{|x_0|^2}^{L^2} [t - |x_0|^2]^{\frac{\alpha}{2}-1} {}_2F_1\left[-\frac{\alpha}{2}, \frac{1}{2}, \frac{1+\alpha}{2}; \frac{t}{L^2}\right] dt, \tag{3}$$

where x_0 is the initial condition, ${}_2F_1(a, b; c; z)$ stands for the hypergeometric function, while $\Gamma(\cdot)$ is the Euler gamma function. From Eqs. (2) and (3), with $\alpha = 2$, one gets

$$\mathrm{CV} = \sqrt{\frac{2}{3}}\sqrt{\frac{L^2 + x_0^2}{L^2 - x_0^2}} = \sqrt{\frac{2}{3}}\sqrt{\frac{1 + (x_0/L)^2}{1 - (x_0/L)^2}}. \tag{4}$$

As Eqs. (2) and (3) imply, the coefficient of variation does not depend on the scale parameter σ. The independence of the CV on the scale parameter σ can be intuitively explained by the fact that σ can be canceled by time rescaling. Such a transformation (linearly) rescales individual FPTs and consequently, in exactly the same way, the MFPT and the standard deviation, making their ratio σ independent. Equation (4) implies that $\mathrm{CV} > 1$ for

$$x_0 \in \left(-L, -\frac{L}{\sqrt{5}}\right) \cup \left(\frac{L}{\sqrt{5}}, L\right), \tag{5}$$

what is in accordance with earlier findings [70].

Equivalently, the setup corresponding to Eqs. (2) and (3) can be described by the Langevin equation,

$$\frac{dx}{dt} = \xi_\alpha(t), \tag{6}$$

and studied by methods of stochastic dynamics. In Eq. (6), the ξ_α is the symmetric α-stable Lévy-type noise and $x(t)$ represents the particle position [with the initial condition $x(0) = x_0$]. The α-stable noise is a generalization of the Gaussian white noise (GWN) to the nonequilibrium realms [73], which, for $\alpha = 2$, reduces to the standard Gaussian white noise. The symmetric α-stable noise is related to the symmetric α-stable process $L(t)$; see Refs. [15,73]. Increments $\Delta L = L(t + \Delta t) - L(t)$ of the α-stable process are independent and identically distributed random variables following an α-stable density with the characteristic function [73,74]

$$\varphi(k) = \langle \exp(ik\Delta L)\rangle = \exp[-\Delta t \sigma^\alpha |k|^\alpha]. \tag{7}$$

Symmetric α-stable densities are unimodal probability densities defined by the characteristic function with probability densities given by elementary functions only in a limited number of cases ($\alpha = 1$ Cauchy density, $\alpha = 2$ Gauss distribution); however, in more general cases, they can be expressed using special functions [75]. The stability index α ($0 < \alpha \leqslant 2$) determines the tail of the distribution, which, for $\alpha < 2$, is of the power-law type, $p(x) \propto |x|^{-(\alpha+1)}$. The scale parameter σ ($\sigma > 0$) controls the width of the distribution, which can be characterized by an interquantile width or by fractional

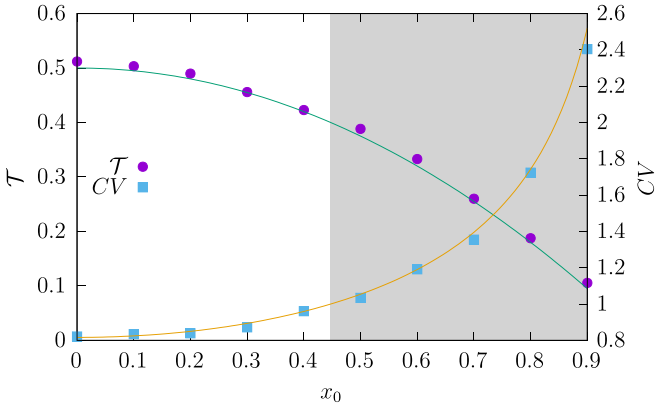

FIG. 1. Numerically estimated MFPT (dots) and CV (squares) as a function of the initial condition x_0 for $\alpha = 2$ along with theoretical values (solid lines). The gray region shows the domain where $\mathrm{CV}(x_0) > 1$.

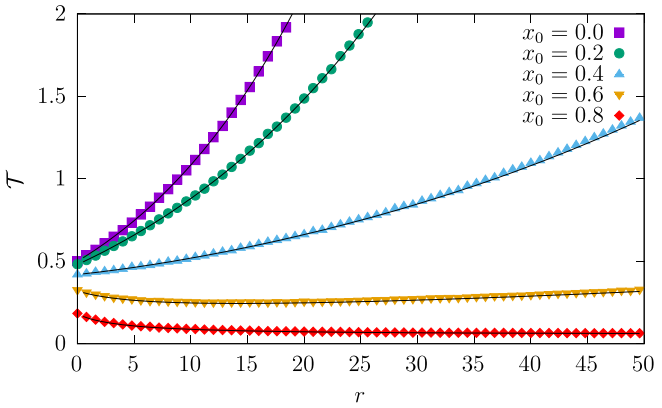

FIG. 2. MFPT under stochastic (Poissonian) restarting for the GWN ($\alpha = 2$) driving as a function of the resetting rate r. Various lines correspond to different initial conditions x_0. Points represent results of numerical simulations, while solid lines represent results of theoretical predictions given by Eq. (10).

moments $\langle |x|^\kappa \rangle$ of the order of κ $(0 < \kappa < \alpha)$, because the α-stable variables with $\alpha < 2$ cannot be quantified by the variance which diverges. Within our studies, we set the scale parameter to unity, i.e., $\sigma = 1$.

The MFPT can be calculated from multiple trajectories generated according to Eq. (6) as the average of the first passage times,

$$\mathcal{T}(x_0) = \langle t_{\mathrm{fp}} \rangle = \langle \inf\{t : x(0) = x_0 \ \wedge \ |x(t)| \geqslant L\} \rangle, \tag{8}$$

while $\mathcal{T}_2(x_0)$ is the second moment of the first passage time. The Langevin equation (6) can be approximated with the (stochastic) Euler-Maruyama method [76,77],

$$x(t + \Delta t) = x(t) + \xi_\alpha^t \Delta t^{1/\alpha}, \tag{9}$$

where ξ_α^t represents a sequence of independent and identically distributed α-stable random variables [78–80]; see Eq. (7).

For the model under study, the coefficient of variation, $\mathrm{CV}(x_0)$, is a symmetric function of the initial condition x_0, i.e., $\mathrm{CV}(x_0) = \mathrm{CV}(-x_0)$, as the escape problem (due to noise symmetry) is symmetric with respect to the sign change in the initial condition x_0. The symmetry is implied from the system symmetry (symmetric boundaries and symmetric noise) and, consequently, is visible not only in Eq. (4), but also in Eqs. (2) and (3). The condition $\mathrm{CV} > 1$ is a sufficient, but not necessary condition when stochastic resetting can facilitate the escape kinetics [81–83]. As Eq. (5) implies, stochastic resetting can accelerate the escape kinetics if the initial condition, which is equivalent to the point from which the motion is restarted, sufficiently breaks the system symmetry, i.e., if restarting the motion anew is more efficient in bringing a particle towards the target (edges of the interval) than waiting for a particle to approach the target (borders). In other words, for the escape from a finite interval, the point from which the motion is restarted is sufficiently far from the center of the interval ($x = 0$). Figure 1 compares the results of numerical simulations (points) with theoretical predictions (solid lines) for $\alpha = 2$ (GWN driving), demonstrating perfect agreement. Due to system symmetry, in Fig. 1, we show results for $x_0 > 0$ only. Moreover, we set the interval half-width L to $L = 1$ and the scale parameter σ to $\sigma = 1$, which is equivalent to the transformation of the escape problem to the dimensionless variables; see the Appendix.

Stochastic resetting, i.e., starting anew from the initial conditions x_0, can be used to facilitate the escape kinetics. One of the common restarting schemes is the so-called fixed rate (Poissonian) resetting, for which the distribution of time intervals between two consecutive resets follows the exponential density $\phi(t) = r \exp(-rt)$, where r is the (fixed) reset rate. Thus, the mean time between two consecutive restarts reads $\langle t \rangle = 1/r$. The MFPT under Poissonian resetting for a process driven by GWN ($\alpha = 2$) [70] from the $(-L, L)$ interval restricted by two absorbing boundaries reads

$$\mathcal{T}(x_0) = \frac{1}{r}\left[\frac{\sinh\frac{2L}{\sqrt{\sigma^2/r}}}{\sinh\frac{L-x_0}{\sqrt{\sigma^2/r}} + \sinh\frac{x_0+L}{\sqrt{\sigma^2/r}}} - 1\right]. \tag{10}$$

Figure 2 presents MFPT as a function of resetting rate r for various initial positions x_0. MFPTs have been estimated using the so-called direct approach [48]. Within such a scheme, from the simulation of the system without resets, the (unknown for $\alpha < 2$) first passage time density is estimated. In the next step, instead of simulating the Langevin dynamics under stochastic resetting, pairs of first passages times (in the absence of resetting) and resetting times are generated until the first passage time is smaller than the resetting time. The first passage time under restart is equal to the sum of (all) generated time intervals between resets increased by the last first passage time; see [48, Fig. 4(a)]. In Fig. 2, points representing the results of computer simulations with $\alpha = 2$ nicely follow solid lines, demonstrating the theoretical predictions given by Eq. (10).

With the help of Eqs. (2) and (3), more general driving than the Gaussian white noise can be studied. As is already visible from Fig. 3(a), which presents numerically estimated $\mathrm{CV}(x_0)$ (points) along with theoretical values (lines), the width of the domain where $\mathrm{CV}(x_0) > 1$ increases with the growing α, i.e., for smaller α, the domain where resetting facilitates the escape kinetics is narrower. The set of initial conditions resulting in facilitation of the escape kinetics is further studied

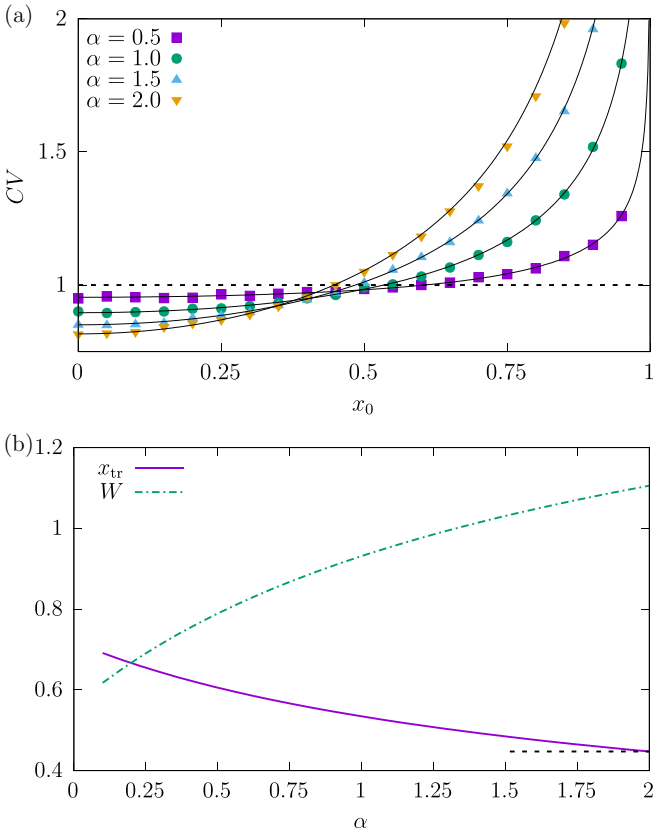

FIG. 3. (a) Numerically estimated $\mathrm{CV}(x_0)$ for $\alpha \in \{0.5, 1.0, 1.5, 2.0\}$ with $L = 1$ (points) complemented by theoretical results (solid lines); see Eqs. (1)–(3). The dashed line shows the $\mathrm{CV} = 1$ level. (b) Numerically calculated $x_{\mathrm{tr}}(\alpha)$ such that $\mathrm{CV}(x_{\mathrm{tr}}) = 1$ (solid line) and the width $W(x_0)$ of the domain where resetting is beneficial (dot-dashed line); see Eq. (11). For $x_0 > x_{\mathrm{tr}}$, the coefficient of variation is greater than 1. The dashed line indicates the GWN limit, i.e., $x_{\mathrm{tr}} = 1/\sqrt{5}$.

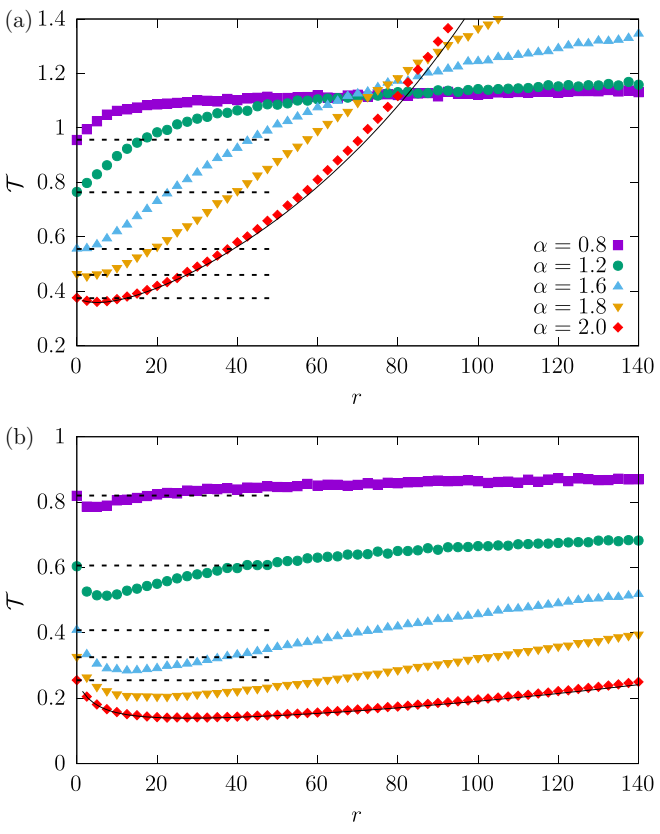

FIG. 4. MFPT under Poissonian resetting. Various points represent different values of the stability index α. The solid line depicts theoretical dependence for $\alpha = 2$ [see Eq. (10)], while dashed lines depict $\mathcal{T}(x_0, r = 0)$ [see Eq. (2)]. The initial condition is set to (a) $x_0 = 0.5$ and (b) $x_0 = 0.7$.

in Fig. 3(b). The bottom panel of Fig. 3 shows x_{tr} such that $\mathrm{CV}(x_{\mathrm{tr}}) = 1$, i.e., x_{tr} divides the set of initial conditions x_0 such that for $|x_0| > x_{\mathrm{tr}}$, the coefficient of variation is greater than 1. From Fig. 3(b), it clearly implies that with the increasing stability index α, the x_{tr} (solid line) moves towards the center of the interval and attains its asymptotic value $1/\sqrt{5}$ for $\alpha = 2$ [see Eq. (5)], which is marked by a dashed line. Moreover, it indicates that under the action of heavy-tailed noises, stochastic resetting can be beneficial in narrower domain of the width W,

$$W = 2 \times (L - x_{\mathrm{tr}}), \tag{11}$$

which, for $L = 1$, is equal to $2(1 - x_{\mathrm{tr}})$; see the dot-dashed line in Fig. 3(b). The monotonous growth of W with the increasing α should be contrasted with the (possible) nonmonotonous dependence of MFPT on α in the absence of resetting (see Eq. (2) and [84]) or for fixed r [see Fig. 4(a)]. The growth of W can be intuitively explained by the mechanism underlying escape dynamics. More precisely, with decreasing α, the dominating escape scenario is the escape via a single (discontinuous) long jump, which is less sensitive to the initial condition than the escape protocol for $\alpha = 2$, when the trajectories are continuous. From Eqs. (2) and (3), one can also calculate the opposite, $\alpha \to 0$, limit of the MFPT, i.e., $\mathcal{T} = 1$, and of the second moment, i.e., $\mathcal{T}_2 = 2$. For $\alpha = 0$, the hypergeometric function in Eq. (3) can be replaced by unity, and the remaining integral reads $\alpha \int_{|x_0|^2}^{L^2} [t - |x_0|^2]^{\frac{\alpha}{2}-1} dt = 2[L^2 - |x_0|^2]^{\frac{\alpha}{2}}$. Additionally, by plugging $\mathcal{T} = 1$ and $\mathcal{T}_2 = 2$ into Eq. (1), one gets $\mathrm{CV} = 1$, regardless of x_0. Indeed, Fig. 3(a) demonstrates that with the decreasing α, the $\mathrm{CV}(x_0)$ curve approaches the $\mathrm{CV} = 1$ line. Consequently, with the decreasing α, the x_{tr} moves to the right, i.e., towards the absorbing boundary. However, we are unable to reliably calculate the $\lim_{\alpha \to 0} x_{\mathrm{tr}}$ as numerical evaluation of the analytical formulas leads to not fully controllable errors. At the same time, for $\alpha \approx 0$, stochastic simulations are unreliable. Overall, we are not able to provide the definitive answer of whether x_{tr} reaches the edges of the interval, i.e., $\pm L$, or stops in a finite distance to the absorbing boundary.

We finish the exploration of LFs under restarting in Fig. 4, which shows numerically estimated MFPTs for LFs as a function of the resetting rate for various values of the stability index α: $\alpha \in \{0.8, 1.2, 1.6, 1.8, 2\}$. The different panels correspond to various initial conditions: (a) $x_0 = 0.5$ and (b) $x_0 = 0.7$. Finally, solid lines show the theoretical dependence for $\alpha = 2$ [see Eq. (10)], while dashed lines $r = 0$ show the asymptotics of MFPTs, i.e., $\mathcal{T}(x_0, r = 0)$ [see Eq. (2)].

First of all, the comparison of Figs. 4(a) and 4(b) further corroborates that with the decreasing α, the domain in which resetting can facilitate the escape kinetics becomes narrower. Importantly, Fig. 4 clearly shows the difference between the escape scenarios for Lévy flights and Brownian motion. For LFs, the dominating strategy, especially for small α, is escape via a single long jump, while for BM, the trajectories are continuous and the particle needs to approach the absorbing boundary. This property changes the sensitivity to resetting, especially in domains where restarting hinders the escape kinetics. For small α, moving back to the initial condition practically does not interrupt waiting for a long jump, while for α close to 2, it substantially decreases the chances of escape. Therefore, for α close to 2, the MFPT grows faster with increasing resetting rate. On the other hand, the growth rate is a decaying function of the initial position; cf. Figs. 4(a) and 4(b) for $\alpha = 2$. Moreover, from the simulations, we do not see the facilitation of the escape kinetics due to resetting in the domain where CV < 1.

In [71], similarities and differences between LFs and LWs have been studied. In particular, it has been demonstrated that for LWs with the power-law distribution of the jump length duration τ,

$$f(\tau) \propto \frac{1}{\tau^{1+\alpha}}, \tag{12}$$

the MFPT from the $(-L, L)$ interval scales as

$$\mathcal{T}(0) \propto \begin{cases} L & \text{for} \quad 0 < \alpha < 1 \\ L^{\alpha} & \text{for} \quad 1 < \alpha < 2 \\ L^{2} & \text{for} \quad \alpha = 2, \end{cases} \tag{13}$$

with the half width of the interval. More precisely, in [71], it was assumed that $v = 1$ and $\tau = |\xi_\alpha|$, where ξ_α are independent and identically distributed random variables following a symmetric α-stable density; see Eq. (7). The observed (asymptotic) scaling suggests that in the situation when the average jump duration (length) becomes finite ($\alpha > 1$), Lévy walks display the same scaling on the interval width as Lévy flights; see Eq. (2). In contrast, for $\alpha < 1$, the FPT for LWs is bounded from below. Namely, the first passage time $t_{\text{fp}} \geqslant L/v$, which originates from the fact that the process has a finite velocity. This property implies that $\mathcal{T}(0) \geqslant L/v$ and thus the scaling of MFPT must differ from $\mathcal{T}(0) \propto L^{\alpha}$ observed for LFs with $\alpha < 1$. Finally, for $\alpha = 2$, the underlying process, by means of the central limit theorem, converges to the Wiener process, revealing the same scaling of the MFPT like a Brownian particle.

III. LÉVY WALKS UNDER STOCHASTIC RESETTING

After studying the properties of LFs on finite intervals under stochastic resetting, we move to the examination of LWs. In the case of LWs, numerical simulations were conducted to investigate the regime in which stochastic resetting can be beneficial. Similarly as in [71], it was assumed that $v = 1$ and $\tau = |\xi_\alpha|$, where ξ_α are independent and identically distributed random variables following a symmetric α-stable density with the scale parameter $\sigma = 1$; see Eq. (7). Therefore, for LWs, we eliminate two of three parameters (v and σ), while we keep the L parameter (see the Appendix), as it allows for the transparent examination of limiting (big number of jumps) behavior.

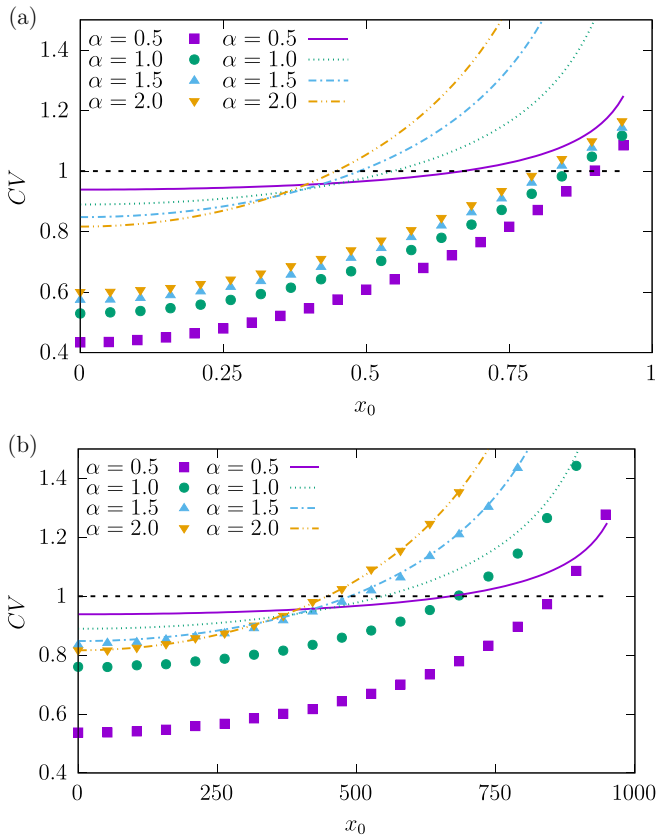

FIG. 5. Coefficient of variation, CV [see Eq. (1)], as a function of the initial position x_0. Points represent the CV for LWs (obtained through numerical simulations) and lines represent the CV for LFs [analytical results from Eqs. (2) and (3)]. Various panels correspond to different values of the interval half-width L: (a) $L = 1$ and (b) $L = 1000$.

For LWs, the first passage time density has two peaks corresponding to escape in a single long jump or a sequence of subsequent jumps towards the left or right boundary. These peaks are located at $(L - x_0)/v$ (escape via the right boundary) or $(x_0 + L)/v$ (escape via the left boundary). The heights of the peaks associated with such escapes increase with the drop in α and decay with the increasing interval half-width L. We suspect that these peaks are one of the reasons for the emergence of differences between LFs and LWs; see, for instance, Eq. (13) for $\alpha < 1$ and the discussion below Eq. (13).

The coefficient of variation, CV(x_0) [48] [see Eq. (1)], obtained through numerical simulations of LWs onto an $(-L, L)$ interval with various initial positions x_0, was compared to the analytical results acquired for LFs; see Eqs. (2) and (3). We focus mainly on the $1 \leqslant \alpha \leqslant 2$ case, as for α from that range, the MFPT as a function of the interval half-width L for LWs and LFs scales in the same manner; see Eqs. (2) and (13). Figure 5(a) demonstrates that for relatively small intervals of half width $[L/(v\sigma) \approx 1]$, the CV for LFs and the CV for LWs noticeably differ, i.e., the CV for LWs is significantly smaller than the CV for LFs. However, as depicted in Fig. 5(b), with increasing L, for the same set of α ($\alpha \in \{1.5, 2\}$), the CV

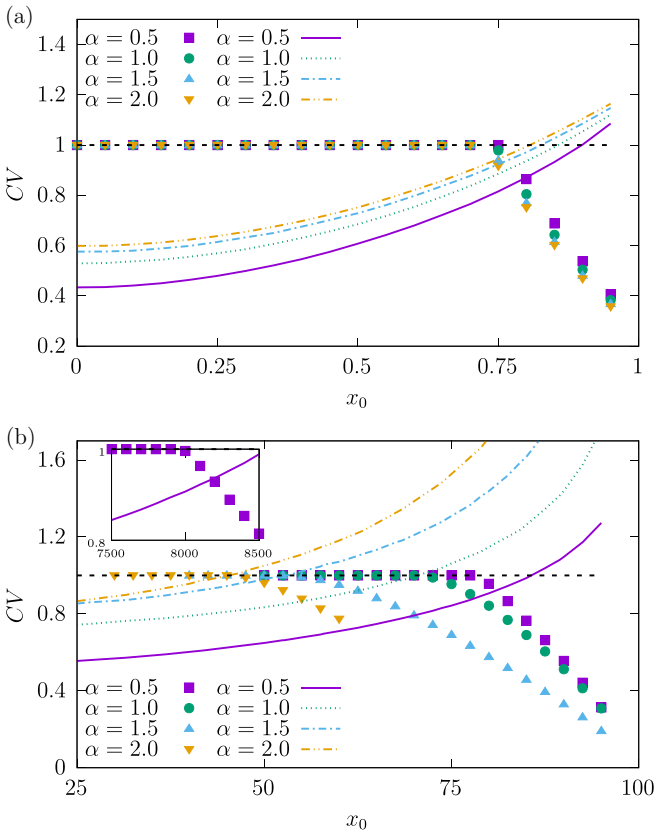

FIG. 6. Numerically estimated (analogous to Fig. 5) coefficient of variation, CV (lines) [see Eq. (1)], as a function of the initial position x_0 for LWs along with the normalized ratio $\Lambda(x_0)$ (points); see Eq. (14). Various panels correspond to different values of the interval half-width L: (a) $L = 1$, (b) $L = 100$, and $L = 10\,000$ [inset in (b)].

for the LWs model follows the one present for LFs. The agreement originates in the fact that for large enough L, the peaks corresponding to escape in a single jump (or sequences of consecutive jumps toward the boundary) in the first passage time distribution are small enough.

In the next step, the region in which stochastic resetting can be beneficial for LWs was explored numerically under a Poissonian (fixed rate) resetting. The distribution of time intervals between two consecutive resets follows the exponential density $\phi(t) = r\exp(-rt)$, where r ($r > 0$) is the reset rate. The efficiency of stochastic resetting can be verified by use of the normalized ratio of the minimal MFPT under stochastic resetting to its value in the absence of resetting,

$$\Lambda(x_0) = \frac{\min_r \mathcal{T}(x_0, r)}{\mathcal{T}(x_0, 0)}, \tag{14}$$

where $\mathcal{T}(x_0, r)$ stands for MFPT under resetting with reset rate r and the initial position x_0 equivalent to the restarting point. If stochastic resetting does not facilitate the escape kinetics, then $\Lambda = 1$ because $\mathcal{T}(x_0, 0)$ is the minimal mean first passage time. The decay of Λ below one indicates that stochastic resetting accelerates the escape kinetics. Figure 6 presents the normalized ratio $\Lambda(x_0)$ (points) along with $\mathrm{CV}(x_0)$ (lines). For small $|x_0/L|$, the asymmetry introduced by the initial position is not strong enough (the restarting point is too close to the origin) to open space for optimization of the MFPT by stochastic resetting, resulting in $\Lambda(x_0) = 1$. Therefore, for small $|x_0|$, $\Lambda(x_0) = 1$ not only shows the impossibility of enhancing the escape kinetics, but also introduces a visual reference level clearly demonstrating where CV drops below unity. From examination of the normalized ratio $\Lambda(x_0)$, it is possible to easily see if the drop in $\Lambda(x_0)$ coincides with the increase of the coefficient of variation, CV, above unity. As expected for $|x_0/L|$ large enough, stochastic resetting facilitates the escape kinetics for LWs. For small L, e.g., $L = 1$ (in physical units $L/(v\sigma) \approx 1$), the region where escape kinetics is accelerated by stochastic resetting differs from the one indicated by the $\mathrm{CV} > 1$ criterion [48] because MFPT can be shortened even in the domain where $\mathrm{CV} < 1$; see Fig. 6(a). This is in accordance with the fact that the condition $\mathrm{CV} > 1$ is sufficient, but not necessary for observation of the facilitation of escape kinetics due to stochastic resetting [81–83]. For large enough interval half-widths L, the point where $\Lambda(x_0)$ drops below unity agrees with the prediction based on the CV criterion for $\alpha \in \{1, 1.5, 2\}$; see Fig. 6(b). However, in the case of $\alpha = 0.5$, the disagreement with the $\mathrm{CV} > 1$ criterion persists. Moreover, for LWs with large L, the coefficient of variation agrees with the one calculated for LFs; see Fig. 5(b).

IV. SUMMARY AND CONCLUSIONS

Lévy flights and Lévy walks constitute two paradigmatic random walk schemes generalizing the Brownian motion. Both for LWs and LFs, displacements are drawn from heavy-tailed distributions with diverging variance. LFs are Markovian processes in which jumps occur at typical time intervals, while LWs include a spatiotemporal coupling between jump lengths and waiting times, penalizing long jumps with long waiting times, making the process non-Markovian. Coupling between jump lengths and waiting times can be linear, resulting in a motion with a constant velocity. Therefore, a random walker in LFs and LWs can be moving along the same turning points, but for LFs, the jumps are instantaneous, while for LWs, a random walker continues motion in a given direction with a constant speed for a given time after which the new direction can be generated. As a consequence, the trajectories of LWs are continuous, while for LFs, they are discontinuous.

We have demonstrated that stochastic resetting can facilitate the escape kinetics, as measured by the mean first passage time, from a finite interval restricted by two absorbing boundaries both for LFs and LWs. Stochastic resetting is beneficial when the initial condition, which is equivalent to the point from which the motion is restarted, sufficiently breaks the system symmetry, i.e., x_0 is sufficiently far from 0 (center of the interval). Under such a condition, restarting the motion anew is more efficient in bringing a particle towards the target than waiting for a particle to approach it. Both for LFs and LWs, the domain in which resetting is beneficial depends on the exponent α defining the power-law distribution of jump lengths. Despite the fact that MFPT can be a nonmonotonous function of stability index α, the width of the domain utilizing restarting is growing with the increasing α, i.e., for lighter

tails, it is wider, as lighter tails change the typical escape scenario.

Lévy flights and Lévy walks display the same scaling of the MFPT on the interval half-width L for $1 \leqslant \alpha \leqslant 2$. For LFs, it is the exact result, while for LWs, it is the large L asymptotics. Analogously, under restarting, for $1 < \alpha \leqslant 2$ with the increasing interval half-width L, the coefficient of variation for LWs tends asymptotically to the one for LFs. Additionally, for LWs with small L, it is clearly visible that the stochastic resetting facilitates escape kinetics, not only in the region where CV > 1, but it can also accelerate the escape kinetics in situations where CV < 1.

The data (generated randomly using the model presented in the paper) that support the findings of this study are available from the corresponding author (B.Ż.) upon reasonable request.

ACKNOWLEDGMENTS

We gratefully acknowledge Poland's high-performance computing infrastructure PLGrid (HPC Centers: ACK Cyfronet AGH) for providing computer facilities and support within computational Grant No. PLG/2024/016969. The research for this publication has been supported by a grant from the Priority Research Area DigiWorld under the Strategic Programme Excellence Initiative at Jagiellonian University.

APPENDIX: DE-DIMENSIONALIZATION OF THE LANGEVIN EQUATION

For LFs, the α-stable noise driven escape from $[-L, L]$ described by the Langevin equation

$$\frac{dx}{dt} = \xi_\alpha(t) = \sigma\xi_\alpha(\sigma = 1; t) \tag{A1}$$

can be studied in dimensionless variables,

$$y = \frac{x}{L} \quad \text{and} \quad s = \frac{t}{T}. \tag{A2}$$

In such variables,

$$\frac{dx}{dt} = \frac{L}{T}\frac{dy}{ds} \tag{A3}$$

and

$$\begin{aligned}\sigma\xi_\alpha &= \sigma\frac{d}{dt}L(sT) = \sigma\frac{ds}{dt}\frac{dL(sT)}{ds} = \frac{\sigma}{T}\frac{d}{ds}[T^{\frac{1}{\alpha}}L(s)] \\ &= \sigma T^{\frac{1}{\alpha}-1}\xi_\alpha(s).\end{aligned} \tag{A4}$$

In the transformation of Eqs. (A1) and (A4), we have used the following facts: (i) the scale parameter σ can be extracted from the noise and used as the multiplicative constant [73], (ii) α-stable noise is the formal time derivative of the α-stable process $L(t)$, and (iii) the α-stable process is $1/\alpha$ self-similar, i.e., $L(Ts) = T^{\frac{1}{\alpha}}L(s)$; see [74]. In new variables, the Langevin equation takes the form

$$\frac{L}{T}\frac{dy}{ds} = \sigma T^{\frac{1}{\alpha}-1}\xi_\alpha(s) \tag{A5}$$

or

$$\frac{dy}{ds} = \frac{\sigma}{L}T^{\frac{1}{\alpha}}\xi_\alpha(s). \tag{A6}$$

Setting $\frac{\sigma}{L}T^{\frac{1}{\alpha}}$ to unity, one finds the characteristic time T,

$$T = \frac{L^\alpha}{\sigma^\alpha}. \tag{A7}$$

In dimensionless variables, the motion is described by the Langevin equation

$$\frac{dy}{ds} = \xi_\alpha(s), \tag{A8}$$

and the motion is continued as long as the particle is within the $[-1, 1]$ interval.

Incorporation of the stochastic resetting (typically) introduces another timescale associated with the inter-resetting intervals. For example, for the fixed rate (Poissonian resetting), time intervals between two consecutive resets follow the exponential density $\phi(t) = r\exp(-rt)$, where r is the (fixed) reset rate. Thus, the mean time between two consecutive restarts reads $\langle t\rangle = 1/r$ and $r = 1/\langle t\rangle$. The dimensionless reset rate $\tilde{r}$ [see Eq. (A2)] reads $\tilde{r} = T/\langle t\rangle$.

Overall, for LFs on a bounded interval accompanied by the stochastic (Poissonian) resetting, the only parameter (in addition to the stability index α determining tails of the jump length distribution) is the dimensionless resetting rate. Alternatively to the above-described transformation of variables, one can set $L = 1$ and $\sigma = 1$. The latter approach is used in the manuscript in the part regarding Lévy flights.

For LWs, the situation is not identical, but very similar to LFs. LWs on a bounded interval $[-L, L]$ are characterized by three parameters: L (interval half-width), v (velocity of propagation), and σ (scale of the jump time and length distribution). Therefore, by rescaling of the type given by Eq. (A2) it is not possible to remove all parameters. After transformation of the variables, a selected parameter must remain. Within current studies, we have decided to keep L, while v and σ are set to unity. Such a selection is motivated by the fact that it is a transparent choice allowing for the study of a regime in which the particle performs many jumps before leaving the domain of motion. Subsequently, it facilitates the use of limit theorems.

[1] M. von Smoluchowski, Ann. Phys. **326**, 756 (1906).
[2] A. Einstein, Ann. Phys. **322**, 549 (1905).
[3] P. Langevin, C. R. Acad. Sci. **146**, 530 (1908).
[4] J. Perrin, Ann. Chim. Phys. **18**, 5 (1909).
[5] H. A. Kramers, Physica **7**, 284 (1940).
[6] N. G. van Kampen, *Stochastic Processes in Physics and Chemistry* (North-Holland, Amsterdam, 1981).
[7] C. W. Gardiner, *Handbook of Stochastic Methods for Physics, Chemistry and Natural Sciences* (Springer Verlag, Berlin, 2009).

[8] *Nonequilibrium Statistical Mechanics*, edited by R. Zwanzig (Oxford University Press, New York, 2001).

[9] W. Horsthemke and R. Lefever, *Noise-inducted Transitions. Theory and Applications in Physics, Chemistry, and Biology* (Springer Verlag, Berlin, 1984).

[10] E. W. Montroll and M. F. Shlesinger, in *Lévy Processes: Theory and Applications*, edited by J. L. Lebowitz and E. W. Montroll (North Holland, Amsterdam, 1984), pp. 1–121.

[11] R. Metzler and J. Klafter, Phys. Rep. **339**, 1 (2000).

[12] R. Metzler and J. Klafter, J. Phys. A: Math. Gen. **37**, R161 (2004).

[13] R. Brown, Philos. Mag. **4**, 161 (1828).

[14] I. Nordlund, Z. Phys. Chem. **87U**, 40 (1914).

[15] A. A. Dubkov, B. Spagnolo, and V. V. Uchaikin, Intl. J. Bifurcation Chaos. Appl. Sci. Eng. **18**, 2649 (2008).

[16] A. V. Chechkin, R. Metzler, J. Klafter, and V. Y. Gonchar, in *Anomalous Transport: Foundations and Applications*, edited by R. Klages, G. Radons, and I. M. Sokolov (Wiley-VCH, Weinheim, 2008), pp. 129–162.

[17] M. F. Shlesinger and J. Klafter, in *On Growth and Form: Fractal and Non-fractal Patterns in Physics*, edited by H. E. Stanley and N. Ostrowsky (Springer Verlag, Berlin, 1986), p. 279.

[18] V. Zaburdaev, S. Denisov, and J. Klafter, Rev. Mod. Phys. **87**, 483 (2015).

[19] S. Denisov, J. Klafter, and M. Urbakh, Physica D **187**, 89 (2004).

[20] J. P. Bouchaud, A. Ott, D. Langevin, and W. Urbach, J. Phys. II France **1**, 1465 (1991).

[21] D. Brockmann, L. Hufnagel, and T. Geisel, Nature (London) **439**, 462 (2006).

[22] D. W. Sims, E. J. Southall, N. E. Humphries, G. C. Hays, C. J. A. Bradshaw, J. W. Pitchford, A. James, M. Z. Ahmed, A. S. Brierley, M. A. Hindell, D. Morritt, M. K. Musyl, D. Righton, E. L. C. Shepard, V. J. Wearmouth, R. P. Wilson, M. J. Witt, and J. D. Metcalfe, Nature (London) **451**, 1098 (2008).

[23] A. M. Reynolds and C. J. Rhodes, Ecology **90**, 877 (2009).

[24] T. A. Amor, S. D. S. Reis, D. Campos, H. J. Herrmann, and J. S. Andrade, Sci. Rep. **6**, 20815 (2016).

[25] J. L. Cabrera and J. G. Milton, Chaos **14**, 691 (2004).

[26] J. J. Collins and C. J. De Luca, Phys. Rev. Lett. **73**, 764 (1994).

[27] T. H. Solomon, E. R. Weeks, and H. L. Swinney, Phys. Rev. Lett. **71**, 3975 (1993).

[28] P. Barthelemy, J. Bertolotti, and D. Wiersma, Nature (London) **453**, 495 (2008).

[29] M. Mercadier, W. Guerin, M. M. Chevrollier, and R. Kaiser, Nat. Phys. **5**, 602 (2009).

[30] E. Barkai, E. Aghion, and D. A. Kessler, Phys. Rev. X **4**, 021036 (2014).

[31] J. P. Bouchaud and A. Georges, Phys. Rep. **195**, 127 (1990).

[32] J. Laherrère and D. Sornette, Eur. Phys. J. B **2**, 525 (1998).

[33] R. N. Mantegna and H. E. Stanley, *An Introduction to Econophysics. Correlations and Complexity in Finance* (Cambridge University Press, Cambridge, 2000).

[34] S. C. Lera and D. Sornette, Phys. Rev. E **97**, 012150 (2018).

[35] T. H. Solomon, E. R. Weeks, and H. L. Swinney, Physica D **76**, 70 (1994).

[36] E. Barkai, Phys. Rev. E **63**, 046118 (2001).

[37] A. V. Chechkin, V. Y. Gonchar, J. Klafter, and R. Metzler, in *Fractals, Diffusion, and Relaxation in Disordered Complex Systems: Advances in Chemical Physics, Part B*, Vol. 133, edited by W. T. Coffey and Y. P. Kalmykov (Wiley, New York, 2006), pp. 439–496.

[38] S. Jespersen, R. Metzler, and H. C. Fogedby, Phys. Rev. E **59**, 2736 (1999).

[39] R. Klages, G. Radons, and I. M. Sokolov, *Anomalous Transport: Foundations and Applications* (Wiley-VCH, Weinheim, 2008).

[40] H. Touchette and E. G. D. Cohen, Phys. Rev. E **80**, 011114 (2009).

[41] H. Touchette and E. G. D. Cohen, Phys. Rev. E **76**, 020101(R) (2007).

[42] A. V. Chechkin and R. Klages, J. Stat. Mech. (2009) L03002.

[43] B. Dybiec, J. M. R. Parrondo, and E. Gudowska-Nowak, Europhys. Lett. **98**, 50006 (2012).

[44] Ł. Kuśmierz, J. M. Rubi, and E. Gudowska-Nowak, J. Stat. Mech. (2014) P09002.

[45] M. R. Evans and S. N. Majumdar, Phys. Rev. Lett. **106**, 160601 (2011).

[46] M. R. Evans, S. N. Majumdar, and G. Schehr, J. Phys. A: Math. Theor. **53**, 193001 (2020).

[47] S. Gupta and A. M. Jayannavar, Front. Phys. **10**, 789097 (2022).

[48] A. Pal and S. Reuveni, Phys. Rev. Lett. **118**, 030603 (2017).

[49] A. Nagar and S. Gupta, Phys. Rev. E **93**, 060102 (2016).

[50] M. Dahlenburg, A. V. Chechkin, R. Schumer, and R. Metzler, Phys. Rev. E **103**, 052123 (2021).

[51] S. Reuveni, Phys. Rev. Lett. **116**, 170601 (2016).

[52] A. Chechkin and I. M. Sokolov, Phys. Rev. Lett. **121**, 050601 (2018).

[53] A. Pal, Ł. Kuśmierz, and S. Reuveni, Phys. Rev. E **100**, 040101(R) (2019).

[54] T. Zhou, P. Xu, and W. Deng, Phys. Rev. E **104**, 054124 (2021).

[55] A. Pal, L. Kuśmierz, and S. Reuveni, Phys. Rev. Res. **2**, 043174 (2020).

[56] A. S. Bodrova and I. M. Sokolov, Phys. Rev. E **101**, 052130 (2020).

[57] J. C. Sunil, R. A. Blythe, M. R. Evans, and S. N. Majumdar, J. Phys. A: Math. Theor. **56**, 395001 (2023).

[58] P. Xu, T. Zhou, R. Metzler, and W. Deng, New J. Phys. **24**, 033003 (2022).

[59] G. M. Viswanathan, M. G. Da Luz, E. P. Raposo, and H. E. Stanley, *The Physics of Foraging: An Introduction to Random Searches and Biological Encounters* (Cambridge University Press, Cambridge, 2011).

[60] V. V. Palyulin, A. V. Chechkin, and R. Metzler, Proc. Natl. Acad. Sci. USA **111**, 2931 (2014).

[61] A. Pal, Phys. Rev. E **91**, 012113 (2015).

[62] T. Zhou, P. Xu, and W. Deng, Phys. Rev. Res. **2**, 013103 (2020).

[63] T. Sandev, V. Domazetoski, L. Kocarev, R. Metzler, and A. Chechkin, J. Phys. A: Math. Theor. **55**, 074003 (2022).

[64] C. Di Bello, A. V. Chechkin, A. K. Hartmann, Z. Palmowski, and R. Metzler, New J. Phys. **25**, 082002 (2023).

[65] S. Redner, *A Guide to First Passage Time Processes* (Cambridge University Press, Cambridge, 2001).

[66] L. Kusmierz, S. N. Majumdar, S. Sabhapandit, and G. Schehr, Phys. Rev. Lett. **113**, 220602 (2014).

[67] V. Méndez, A. Masó-Puigdellosas, T. Sandev, and D. Campos, Phys. Rev. E **103**, 022103 (2021).

[68] Ł. Kuśmierz and E. Gudowska-Nowak, Phys. Rev. E **92**, 052127 (2015).

[69] A. Stanislavsky and A. Weron, Phys. Rev. E **104**, 014125 (2021).
[70] A. Pal and V. V. Prasad, Phys. Rev. E **99**, 032123 (2019).
[71] B. Dybiec, E. Gudowska-Nowak, E. Barkai, and A. A. Dubkov, Phys. Rev. E **95**, 052102 (2017).
[72] R. K. Getoor, Trans. Amer. Math. Soc. **101**, 75 (1961).
[73] A. Janicki and A. Weron, *Simulation and Chaotic Behavior of α-stable Stochastic Processes* (Marcel Dekker, New York, 1994).
[74] G. Samorodnitsky and M. S. Taqqu, *Stable Non-Gaussian Random Processes: Stochastic Models with Infinite Variance* (Chapman and Hall, New York, 1994).
[75] K. Górska and K. A. Penson, Phys. Rev. E **83**, 061125 (2011).
[76] D. J. Higham, SIAM Rev. **43**, 525 (2001).
[77] R. Mannella, Intl. J. Mod. Phys. C **13**, 1177 (2002).
[78] J. M. Chambers, C. L. Mallows, and B. W. Stuck, J. Am. Stat. Assoc. **71**, 340 (1976).
[79] A. Weron and R. Weron, Lect. Notes Phys. **457**, 379 (1995).
[80] R. Weron, Stat. Prob. Lett. **28**, 165 (1996).
[81] T. Rotbart, S. Reuveni, and M. Urbakh, Phys. Rev. E **92**, 060101(R) (2015).
[82] A. Pal and V. V. Prasad, Phys. Rev. Res. **1**, 032001(R) (2019).
[83] A. Pal, S. Kostinski, and S. Reuveni, J. Phys. A: Math. Theor. **55**, 021001 (2022).
[84] K. Szczepaniec and B. Dybiec, J. Stat. Mech. (2015) P06031.